Influence of Dipolar Interaction on Vortex Dynamics in Arrays of Ferromagnetic Disks

Andreas Vogel,[1,*] André Drews,[1,2] Thomas Kamionka,[1] Markus Bolte,[1,2] and Guido Meier[1]

[1]*Institut für Angewandte Physik und Zentrum für Mikrostrukturforschung, Universität Hamburg, Jungiusstrasse 11, 20355 Hamburg, Germany*

[2]*Arbeitsbereich Technische Informatik Systeme, Universität Hamburg, Vogt-Kölln-Strasse 30, 22527 Hamburg, Germany*

(Received 12 December 2009; revised manuscript received 25 May 2010; published 12 July 2010)

The influence of the magnetostatic interaction on vortex dynamics in arrays of ferromagnetic disks is investigated by means of a broadband ferromagnetic-resonance setup. Transmission spectra reveal a strong dependence of the resonance frequency of vortex-core motion on the ratio between the center-to-center distance and the element size. For a decreasing ratio, a considerable broadening of the absorption peak is observed following an inverse sixth power law. An analogy between the vortex system and rotating dipoles is confirmed by micromagnetic simulations.

DOI: 10.1103/PhysRevLett.105.037201 PACS numbers: 75.75.−c, 75.25.−j, 75.40.Gb, 76.50.+g

Vortex dynamics can be observed in many physical systems such as ferromagnets, superconductors, and Bose-Einstein condensates. Explanations of flow phenomena in modern fluid mechanics are often predicated on the dynamics of vortices. In recent years, small ferromagnetic structures with vortex magnetization configuration have gained intense scientific interest because of their dynamics on the subnanosecond time scale and potential technological applications, such as ultrafast and high-density digital storage devices [1–4]. Even medical applications have lately been discussed [5]. Understanding the influence of the various internal and external parameters on the dynamic properties of the magnetic vortex is an important issue for further development. The gyrotropic mode and switching of single vortex cores have been studied intensely [6–10]. However, investigation of the interaction between several vortices [11–14] is still required. Coupling of magnetic vortices, e.g., provides a model system in fundamental research and could also determine the packing density in storage devices.

To describe the magnetic behavior of an array of ferromagnetic disks, the magnetostatic interaction between single elements has to be considered when the interelement distance is less than the lateral size of one disk [15]. An increase of the initial susceptibility and a decrease of the vortex nucleation and annihilation fields are observed [16]. Analytical and numerical calculations using the rigid vortex model predict a shift of the eigenfrequency of vortex-core motions in adjacent ferromagnetic disks depending on the core polarizations and the distance between the disk centers [11,17].

Here, we experimentally study the influence of the magnetostatic interaction on the resonance frequency of vortices trapped in arrays of $4 \times N$ ferromagnetic disks by varying the distance and the size of the elements. Energy absorption in radio-frequency magnetic fields has been determined via a broadband ferromagnetic-resonance (FMR) setup using a vector-network analyzer. The vortex resonance frequency strongly depends on the magnetostatic coupling within the array. The relative broadening of the absorption peak due to resonant vortex-core motion varies with the inverse sixth power of the normalized center-to-center distance. This kind of distance dependence is a prominent feature of the fundamental van der Waals type interactions. An analogy can be illustrated considering the interaction of rotating dipoles whose magnetic moments are affected by the stray fields of the neighbors.

Arrays of ferromagnetic disks ($N \approx 300$) as shown in Fig. 1(a) are fabricated using electron-beam lithography and lift-off processing. Polycrystalline permalloy ($Ni_{80}Fe_{20}$) with a thickness of $L = 50$ nm is thermally evaporated onto a 100 nm thin silicon-nitride membrane.

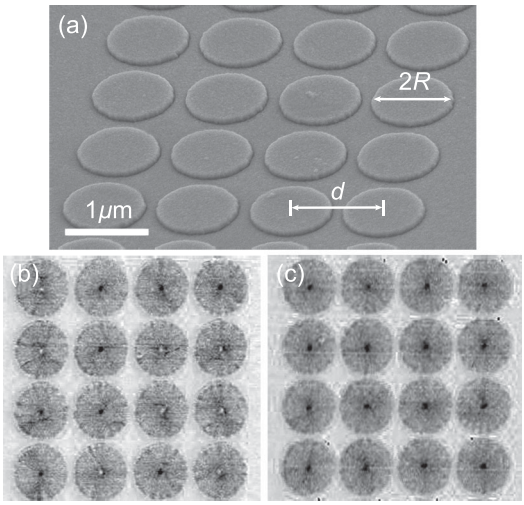

FIG. 1. (a) Scanning-electron micrograph of a $4 \times N$ array of permalloy disks with a radius of $R = 500$ nm and a center-to-center distance of $d = 1.2$ μm under the signal line of a coplanar waveguide. Magnetic force micrographs of an array with $d = 1.1$ μm after applying an additional perpendicular bias field of (b) 0 mT and (c) $\mu_0 H_z \approx 70$ mT.

For a disk radius of $R = 500$ nm, the center-to-center distance d is varied from 1.1 μm to 1.6 μm. Furthermore, the radius R is varied from 300 nm to 500 nm at a constant center-to-center distance $d = 1.1$ μm. A coplanar waveguide is deposited on top of the disks via dc magnetron sputtering of 125 nm gold. The signal line of the waveguide tapers down to 7 μm.

Vortex configurations are characterized by their polarization $p = \pm 1$ and their chirality $C = \pm 1$. The polarization p indicates the magnetization direction of the core and the chirality describes the clockwise ($C = -1$) or counterclockwise ($C = 1$) in-plane curling of the magnetization around the core. Magnetic force micrographs confirm the presence of magnetic vortex cores in the center of each disk. Figure 1(b) reveals that the polarization p is statistically distributed. To reset the vortex magnetization configuration, an in-plane bias field $\mathbf{H}_0$ is alternately reduced starting from saturation. A perpendicular bias field $\mathbf{H}_z$ in addition to the in-plane field can lead to a preferred magnetization direction of the cores; see Fig. 1(c). Using magnetic transmission soft x-ray microscopy [18], the chirality C has been confirmed to be statistically distributed as well (not shown).

Transmission spectra are measured at room temperature [19]. The 1 mW sinusoidal signal causes a radio-frequency magnetic field $\mathbf{H}_{\mathrm{rf}}(t)$ of up to 0.4 mT around the central conductor predominantly acting in the plane of the disks. A static external bias field $\mathbf{H}_0$ is applied parallel to the waveguide. Figure 2(a) shows FMR transmission spectra of an array of permalloy disks taken at different bias fields from $\mu_0 H_0 = -40$ mT to 40 mT. Prior to each frequency sweep, the disks are reset.

In the case of a time-dependent external magnetic field the vortex core gyrates on an elliptical trajectory around its equilibrium position where the rotational direction depends on the polarization p. The observed reduction of transmission in the FMR spectra originates from energy absorption in the gyrotropic mode. At zero bias field, the frequency $f_0 \approx 355$ MHz of minimum transmission in Fig. 2(b) almost coincides with the results of an analytical theory and micromagnetic simulation of the eigenfrequency of resonant circular vortex-core motion [20] for a single disk with an aspect ratio $L/R = 0.1$ corresponding to our sample ($L = 50$ nm and $R = 500$ nm). An in-plane bias field leads to a translation of the equilibrium position of the vortex core away from the center of the disk. We observe a shift of the resonance peak of up to 13% for increasing bias field until vortex annihilation occurs. Within the analytical model of a two-dimensional oscillator [8] this significant dependence could be explained by an anharmonic contribution to the magnetic potential of the disk. A considerable broadening of the resonance peak at zero bias field is observed for decreasing center-to-center distance d; see Figs. 2(b)–2(d).

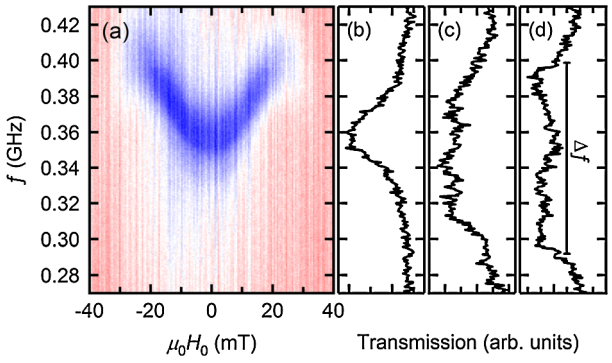

FIG. 2 (color online). (a) FMR transmission spectra of an array of permalloy disks ($R = 500$ nm and $d = 1.6$ μm). The bias field along the signal line is successively increased from $\mu_0 H_0 = -40$ mT to 40 mT. The dark (blue) color corresponds to reduced transmission. Spectra at zero bias field for a center-to-center distance of (b) $d = 1.6$ μm, (c) $d = 1.2$ μm, and (d) $d = 1.1$ μm are shown.

The linewidth of the absorption peak in FMR spectra of thin films is proportional to the resonance frequency and depends on the intrinsic Gilbert damping parameter α and magnetic inhomogeneities [21,22]. For a single disk, the linewidth of the vortex resonance can be expressed as $\Delta f = 2 f_0 \alpha [1 + \ln(R/R_c)/2]$ [23], where R_c is the thickness-dependent vortex core radius. Scanning transmission x-ray microscopy reveals variations of f_0 in the order of half of the linewidth between single elements with nominally equal shape [24]. The minimum linewidth Δf_{min} in our measurements arises from the superposition of resonances of the single elements within the array. We attribute the relative broadening $(\Delta f - \Delta f_{\mathrm{min}})/f_0$ in Figs. 2(b)–2(d) to a spread of resonance frequencies due to magnetostatic coupling within the array.

An off-centered vortex core breaks the rotational symmetry of the disk i resulting in the formation of magnetic charges $\sigma(\varphi_i) = \mathbf{m}(\varphi_i) \cdot \mathbf{n}$ at its side surface [11] with the local magnetic moment $\mathbf{m}(\varphi_i) = \mathbf{M}(\varphi_i)/M_s$, the polar angle φ_i, and the surface normal $\mathbf{n}$. The magnetostatic energy, as a function of the position $\mathbf{a}_i = \mathbf{X}_i/R$ of the ith vortex core with respect to the center of the disk i

$$E_m(\mathbf{a}_i) = \frac{\mu_0 M_s^2}{8\pi} \int dS \int dS' \frac{\sigma(\varphi_i)\sigma(\varphi_i')}{|\mathbf{r}_i - \mathbf{r}_i'|}, \qquad (1)$$

can be calculated by integration over the disk's side surface. Contributions of magnetic charges at the top and at the bottom surface are neglected. Provided that the vortex-core displacement is small in comparison to the disk radius ($|\mathbf{a}_i| \ll 1$), the self-magnetostatic energy can be expanded in a series on the displacement $|\mathbf{a}_i|$. At zero bias field, the total energy of a vortex trapped in the disk i within the array can be written as

$$E_i(\mathbf{a}_i, \mathbf{a}_j) = \frac{\kappa}{2}|\mathbf{a}_i|^2 + E_{\mathrm{rf}}(\mathbf{a}_i) + \sum_{j \neq i} E_{\mathrm{int}}(\mathbf{a}_i, \mathbf{a}_j), \qquad (2)$$

setting the equilibrium energy $E(0)$ for a centered vortex core ($|\mathbf{a}_i| = 0$) to zero. The first term represents the sum of the exchange energy and self-magnetostatic energy of a

single off-centered vortex core, where the stiffness constant κ is a function of the thickness, the radius, and the saturation magnetization M_s of the disk [16]. The second term in Eq. (2) $E_{\mathrm{rf}}(\mathbf{a}_i) = -C_i\mu_0 M_s \pi R^2 L H_{\mathrm{rf}}(t) a_{iy}$ is the approximated Zeeman energy in the radio-frequency field $\mathbf{H}_{\mathrm{rf}}(t) = H_{\mathrm{rf}}(t)\mathbf{e}_x$ around the central conductor of the coplanar waveguide. The third term is the sum over the energy contributions $E_{\mathrm{int}}(\mathbf{a}_i, \mathbf{a}_j)$ due to magnetostatic interaction with the surrounding disks j in the array.

To numerically calculate the magnetostatic energy between the side surfaces of two neighboring disks i and j, Eq. (1) has to be modified by substituting φ_j and $\mathbf{r}_j$ for φ_i' and $\mathbf{r}_i'$, respectively. Since the core radius R_c is small in comparison to the disk radius R, the contribution of the magnetic charges stored at the vortex core is negligibly small even for center-to-center distances $d \approx 2R$. Shibata *et al.* numerically found an inverse sixth power dependence of the time-averaged magnetostatic energy on the normalized center-to-center distance [11].

Micromagnetic simulations for small displacements of the vortex core confirm that the stray field of a ferromagnetic disk corresponds to the field of a magnetic dipole located in the center of the disk; see Fig. 3. Simulations of a disk with $L = 50$ nm and $R = 500$ nm were performed using the Object Oriented MicroMagnetic Framework (OOMMF) [25] with a cell size of $4 \times 4 \times 50$ nm^3. Typical material parameters of permalloy, i.e., $M_s = 8 \times 10^5$ A/m, an exchange constant $A = 13 \times 10^{-12}$ J/m, and $\alpha = 0.01$ are assumed. The direction of the average magnetization vector in the radio-frequency magnetic field $\mathbf{H}_{\mathrm{rf}}(t)$ is independent of the sign of the chirality C; compare Figs. 3(a) and 3(b). In both cases, the field $\mathbf{H}_{\mathrm{rf}}(t)$ leads to an enlargement of a domain in the same direction. The phase shift of 180° between the vortex cores does not significantly influence the resulting stray field. An analogy can be drawn between an array of disks and rotating dipoles. The relative rotational direction of the average magnetization vectors and hence the time-dependent direction of the stray fields is determined by the vortex-core polarization p. It is not adequate to consider the interaction energy between the disks i and j as the energy of permanent dipole moments in their stray fields ($\propto d_{ij}^{-3}$). The magnetic dipoles are nonpermanent since the magnitude of the vortex-core displacement $\mathbf{a}$ is not fixed but determined via the balance between Zeeman energy, exchange energy, and magnetostatic energy. Changes in the average magnetization vectors are induced depending on the strength and the direction of the stray fields. Induced dipoles obey an inverse sixth power dependence of the magnetostatic interaction energy on the center-to-center distance. Taking into account numerical calculations using the modified Eq. (1), the energy contribution due to magnetostatic interaction can be expressed as

$$E_{\mathrm{int}}(\mathbf{a}_i, \mathbf{a}_j) = \frac{C_i C_j}{(d_{ij}/R)^6}(\eta_{ijx} a_{ix} a_{jx} - \eta_{ijy} a_{iy} a_{jy}). \quad (3)$$

Here, the parameters η_{ijx} and η_{ijy} are a measure for the symmetry of the stray fields and depend on the orientation of the vector between the disks i and j. In the radio-frequency field $\mathbf{H}_{\mathrm{rf}}(t)$, both components of the displacements $\mathbf{a}_i(t)$ and $\mathbf{a}_j(t)$ depend on the chiralities C_i and C_j, respectively. Thus, the energy $E_{\mathrm{int}}(\mathbf{a}_i, \mathbf{a}_j)$ finally does not depend on C_i and C_j as expected for the rotating dipoles. Since $\mathbf{H}_{\mathrm{rf}}(t)$ is applied in x direction, only the x components of $\mathbf{a}_i(t)$ and $\mathbf{a}_j(t)$ are affected by the polarizations p_i and p_j.

Assuming an unchanged static structure of the vortex, the dynamics can be described using the Thiele equation. The equation of motion of the ith vortex core can be written as [26]

$$\mathbf{F}_i + \mathbf{G}_i \times \mathbf{v}_i + D\mathbf{v}_i = 0, \quad (4)$$

where $\mathbf{F}_i = -\nabla E_i$ is the force acting on the core, $\mathbf{G}_i = -G_{0i}\mathbf{e}_z = -(2\pi\mu_0 M_s L p_i/\gamma)\mathbf{e}_z$ is the gyrovector with the gyromagnetic ratio γ, $\mathbf{v}_i = R \cdot d\mathbf{a}_i(t)/dt$ is the velocity, and $D = -2\pi\alpha\mu_0 M_s L[1 + \ln(R/R_c)/2]/\gamma$ is a damping parameter. Equation (4) describes two-dimensional damped coupled oscillations driven by a time-dependent external force. Considering two disks i and j within the array and neglecting the damping ($D = 0$), we obtain an expression for the shift of the eigenfrequency of the ith vortex core due to magnetostatic interaction between disk i and j from the above Eqs. (2)–(4):

$$\frac{f_i}{f_0} = 1 + \frac{1}{2\kappa}\left(\frac{d_{ij}}{R}\right)^{-6}(p_i p_j \eta_{ijx} - \eta_{ijy}), \quad (5)$$

where $f_0 = \kappa/(2\pi R^2 |G_{0i}|)$. The frequency has been expanded in a series about f_0 and only linear terms in η_{ijx} and η_{ijy} are taken into account. Note that a part of the frequency shift in Eq. (5) is independent of the core polarizations p_i and p_j and therefore only depends on the stiffness constant κ and the normalized center-to-center distance d_{ij}/R as well as the orientation of the vector between the disks i and j. The total shift of the eigenfre-

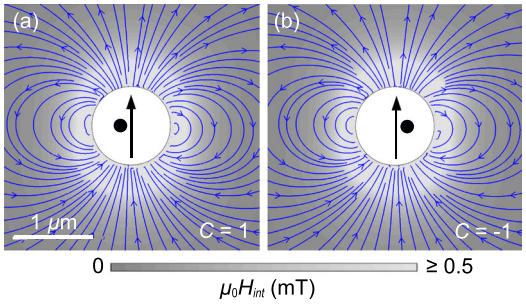

FIG. 3 (color online). Micromagnetic simulation of the stray field of disks with off-centered vortex cores. Arrows outside the disk represent streamlines of the stray field. The black arrow in the disk shows the direction of the in-plane average magnetization vector and the black point is a sketch of the relative position of the core in case of (a) $C = +1$ and (b) $C = -1$.

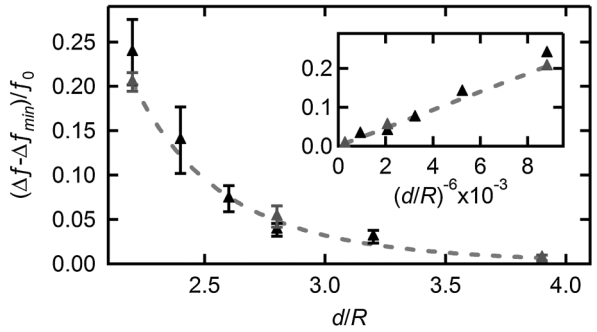

FIG. 4. Relative broadening $(\Delta f - \Delta f_{\min})/f_0$ of the absorption peak in the FMR spectra at zero bias field versus normalized center-to-center distance d/R for various arrays of permalloy disks. Black and gray triangles depict mean values of the experimental data for different distances and different element sizes, respectively. The dashed line marks an inverse sixth power law $\Delta\eta' \cdot (d/R)^{-6}$ with $\Delta\eta' = 23.32 \pm 1.01$. The inset shows the same data plotted as function of $(d/R)^{-6}$.

quency due to magnetostatic interaction with all surrounding disks j within an array can be described via an effective parameter η_i': $f_i/f_0 = 1 + \eta_i'(d/R)^{-6}$.

Figure 4 depicts the mean values of the experimentally observed relative broadenings $(\Delta f - \Delta f_{\min})/f_0$ of the absorption peak in the transmission spectra at zero bias field as a function of the normalized center-to-center distance d/R. The experimental data reveal a relative broadening of more than 20% for $d/R = 2.2$. In accordance with the frequency shift due to magnetostatic interaction, it turns out to decrease following an inverse sixth power law which is illustrated by the dashed line.

The effective parameter η_i' introduced to describe the frequency shift of an element i within the array varies depending on the distribution of the core polarization and the dimensions of the array. Unequal numbers of nearest neighbors in the center, in comparison to the border of the array, lead to variations of η_i' as well. This results in a spread $\Delta\eta'(d/R)^{-6}$ of resonance frequencies observed as relative broadening in the FMR transmission spectra. By changing the normalized center-to-center distance d/R, we experimentally observe the characteristic dependence following an inverse sixth power law. Experiments varying the radius R of the disks underline the universal dependence on d/R since they can be fitted without changing the parameter $\Delta\eta'$.

We have shown via magnetic force microscopy that the core polarization is statistically distributed within the arrays investigated in the FMR measurements. It turns out that applying a perpendicular bias field of $\mu_0 H_z \approx 70$ mT during the reset to the vortex configuration [compare Figs. 1(b) and 1(c)] does not lead to a significant change in the relative broadening (not shown). Hence, the polarization-independent contributions to the effective parameter η_i' are dominant in this case.

In summary, a strong dependence of the resonance frequency of vortex-core motion on the magnetostatic coupling within an array has been experimentally demonstrated. An analogy can be drawn between the vortex system and an array of rotating induced dipoles which illustrates the proportionality of the frequency shift to the inverse sixth power of the normalized center-to-center distance. Since the resonance frequency is a fundamental parameter for vortex dynamics, it is mandatory to consider this dependency in technological applications.

We would like to thank L. Bocklage and V. Novosad for fruitful discussions, J. Topp, M.-Y. Im, and P. Fischer for excellent support with the measurement setups, U. Merkt for continuous support and fruitful discussions, and M. Volkmann for superb technical assistance. Financial support of the Deutsche Forschungsgemeinschaft via the Sonderforschungsbereich 668 and the Graduiertenkolleg 1286 as well as the Hamburger Landesexzellenzinitiative via the Exzellenzcluster ''Nano-Spintronik'' is gratefully acknowledged. Operation of the x-ray microscope is supported by the DOE, Office of Science, under Contract No. DE-AC02-05-CH11231.

*andreas.vogel@physnet.uni-hamburg.de

[1] T. Shinjo *et al.*, Science **289**, 930 (2000).
[2] R. P. Cowburn *et al.*, Phys. Rev. Lett. **83**, 1042 (1999).
[3] R. Antos, Y. Otani, and J. Shibata, J. Phys. Soc. Jpn. **77**, 031004 (2008).
[4] S. Bohlens *et al.*, Appl. Phys. Lett. **93**, 142508 (2008).
[5] D.-H. Kim *et al.*, Nature Mater. **9**, 165 (2010).
[6] C. E. Zaspel *et al.*, Phys. Rev. B **72**, 024427 (2005).
[7] B. Van Waeyenberge *et al.*, Nature (London) **444**, 461 (2006).
[8] B. Krüger *et al.*, Phys. Rev. B **76**, 224426 (2007).
[9] K. Yu. Guslienko, K.-S. Lee, and S.-K. Kim, Phys. Rev. Lett. **100**, 027203 (2008).
[10] M. Bolte *et al.*, Phys. Rev. Lett. **100**, 176601 (2008).
[11] J. Shibata, K. Shigeto, and Y. Otani, Phys. Rev. B **67**, 224404 (2003).
[12] K. S. Buchanan *et al.*, Nature Phys. **1**, 172 (2005).
[13] T. Kimura *et al.*, Appl. Phys. Lett. **90**, 132501 (2007).
[14] Y. Liu *et al.*, Phys. Rev. B **79**, 104435 (2009).
[15] G. Gubbiotti *et al.*, J. Appl. Phys. **99**, 08C701 (2006).
[16] K. Yu. Guslienko *et al.*, Phys. Rev. B **65**, 024414 (2001).
[17] J. Shibata and Y. Otani, Phys. Rev. B **70**, 012404 (2004).
[18] P. Fischer *et al.*, Mater. Today **9**, 26 (2006).
[19] J. Podbielski, F. Giesen, and D. Grundler, Phys. Rev. Lett. **96**, 167207 (2006).
[20] V. Novosad *et al.*, Phys. Rev. B **72**, 024455 (2005).
[21] R. Urban *et al.*, Phys. Rev. B **65**, 020402(R) (2001).
[22] R. D. McMichael, D. J. Twisselmann, and A. Kunz, Phys. Rev. Lett. **90**, 227601 (2003).
[23] K. Yu. Guslienko, Appl. Phys. Lett. **89**, 022510 (2006).
[24] T. Kamionka *et al.* (to be published).
[25] http://math.nist.gov/oommf/.
[26] A. A. Thiele, Phys. Rev. Lett. **30**, 230 (1973).